ISSN: 0974-5823 Vol. 7 No. 2 February, 2022

International Journal of Mechanical Engineering

Preparation and investigation of aluminum alloys (Al-Zn-Mg-Ti) and (Al-Zn-Mg-Mn) for use in radiation shields

Sukaina Iskandar Yusuf * [1] , Thuraya Yarb Sabri [1]

[1] Department of Physical, Science college, Tikrit University,Salah Al-Deen, Iraq

*Corresponding author:

Abstract. In our current study, two aluminum alloys were prepared, which are alloy A (Al-Zn-Mg-Ti) and alloy B (Al-Zn-Mg-Mn), and the possibility of manufacturing radiation-protective shields was studied, including an alternative to lead, by conducting several tests on them. The possibility of X-ray attenuation was studied using these alloys, where the results gave a linear behavior between the absorbance and thickness, as well as for each free path rate and half thickness, while the behavior was inverse between (μ, μ_m) with the alloys thickness under study. Alloy A gave better results than alloy B in attenuating X-rays This is due to the result of adding (Ti) to the alloy A, but this does not mean that Alloy B had no role in attenuating X-rays, but that its attenuation rate was less than Alloy A.

Keywords. Aluminum alloys, Free path rate, Half thickness, Radiation-protective shields, X-ray attenuation.

Introduction

Humans have a negative view of nuclear applications, even peaceful ones, because of the harm ionizing radiation may do, and this is widely accepted.

The great confinement power of lead makes it an excellent choice for X-ray protective shields in hospitals, clinics, and nuclear plants because of the enormous regions it can protect while maintaining the same level of protection as other materials. Protection barriers are getting stronger with concrete and other building materials as the price of lead increases. Therefore, research continued to find alternative methods and materials for the manufacture of radiation shields [1,2].

The lined and mass attenuation factors of some structure materials were studied using radioactive sources (^{60}Co, ^{137}Cs, and ^{133}Ba) with energies (81, 356, 662, 1173, 1332), respectively, and it was discovered that granite is one of the best structure materials for use in shielding against gamma rays. While it was discovered that thermiston was less able to attenuate due to its very low density and low concentration of elements with a high atomic number [2].

Another study looked at (μ_m) and half thickness of some polymer and plastic materials using gamma-ray interaction simulations with the material using Monte Carlo Cod. For gamma rays above, it was discovered that the radio-chromium dye film (nylon base) has better shielding efficacy than concrete (100Kv) [3].

Instead of using tempering coefficients, researchers analyzed half-thickness HVL and tenth-value TVL to conduct sheltering calculations for concrete with varied densities. It turns out that when concrete density raises, HVL and TVL values fall, meaning that γ-ray energy can be decreased by increasing shielding material density and indirectly decreasing material HVL and TVL thickness [4].

To find out how much quantity X-rays lose after hitting barite concrete, researchers used a range of different-sized samples. Experimental observations related to theoretical standards derived from XCOM simulation program showed that results from the two methods for the identical material employed in this study coincided, and it was established that density contributes to photon attenuation coefficients [5].

It was found that μ and μ_m of the gamma-rays could be computed theoretically using Win-XCOM simulation software by employing baro-bismuth-borosilicate glass samples. In particular, the 25% Bi2O3-containing transparent mixed oxides of heavy metals offer good gamma ray shielding qualities [6].

Study of(μ, μ_m and $X_{1/2}$) gamma-rays from radioactive sources (226Ra, 133Ba) using several types of Egyptian timber. Investigators detected a high correlation of timber density with both (μ and μ_m) finding that the attenuation factor is oppositely correlated to the energy of the timber in question. Photon has an inverse relationship with timber density. Investigators found that Aro timber, the type utilized in this study, is better suited for making γ-ray protecting than the other timbers they tested [7].

For the X-ray investigates, poly-ethylene polymer low density was use and oyster shell powder was added in various weight percentages. The free path rate is inversely related to the same weight ratios of the composite under examination [8].

A study on (Al, Pb, and Pb-glass) shields using Co^{60} and Cs^{137} revealed that the dose rate is controlled by the atomic number of the shield material, with the glazed lead shield (Pb-glass) having higher absorbency than the other shields [9].

The relationship between the intensity of the incident ray (I) and the incident ray (I_0) is described by the Beer-Lambert Law, which states [3,7,10,11]:

$I = I_0 [\exp(-\mu x)]$ 1

Which :

X : Permeability distance into the material

μ : Linear attenuation coefficients

The coefficient of mass attenuation is equal to (μ/ρ) in the relationship between the coefficient of linear attenuation and the density [3,7]

$$\mu_m = [\mu/\rho] = [(-\frac{1}{\rho_x}) ln (\frac{I}{I_0})] \quad \text{.....2}$$

ρ_x : the density .

(μ) is a characteristic of the attenuated medium and the X-ray energy employed. The free path rate (λ) of a photon, which may be computed using the following mathematical connection [12]:

$$\lambda = [1/\mu] \quad \text{.....3}$$

There is a material layer known as the "Half Value Layer," which suppresses the incident ray's intensity by half. By using this mathematical relationship [3,4,7], we may figure out how much material must be added in order to lessen the passing rays' intensity by half.

$$X_{(0.5)} = [(ln2)/\mu] \quad \text{..... 4}$$

Statistics:

Standard Deviation :

The total number of detectors fluctuates statistically, indicating that hardware and human factors influence the measurement and detection process. To ensure the highest level of accuracy, we look for statistics in these measurements. The standard deviation can be calculated using the following relationship [13] :

$$\sigma_x = \sqrt{\frac{\sum_{i=1}^{n}(\bar{X}-X_i)^2}{n-1}} \quad \text{.....5}$$

$\bar{X}$: Arithmetic mean (N) of individual measurements .

X_i : Single Measurements .

$$R.S.D = [\frac{\sigma_x}{\bar{X}}] \times 100\ \% \quad \text{.....6}$$

Which

R.S.D. : Relative Standard Deviation

In our current work, two aluminum alloys, were created, and the possibility of making radiation-protective shields, including an alternative to lead, was investigated by conducting many tests on them.

Experimental procedures

Alloys preparation

At 700°C, aluminum was placed in a furnace with digital control of German origin, type (Nabertherm), and passed through a digital scale with an accuracy of (0.1) mg in order to limit the weight ratios utilized in creating alloys A and B, Table 1. In order to keep each element from oxidation or combustion, the remaining alloying components were added gradually by tongs after the metal had completely melted and was completely insulated from oxygen.

An electric mixer set to 150 radians per minute swirled the molten to ensure uniformity. An oven-heated carbon mold was used to pour the molten metal inside and allow it to cool slowly. Both alloys were made using this technique. It was possible to collect cylindrical samples of 1 cm in diameter by 10 cm in length. The samples were cut with an electric cutting device of Chinese origin, type (METKON), and the thickness was measured with a digital vernier of Japanese origin, type (METKON) (Fowler).

Table 1. The mass-to-weight ratios of the casting elements.

Alloys	Al%	Zn%	Mg%	Ti%	Mn%
A	91.5	7.1	0.54	0.55	----
B	91.5	7.1	0.54	----	0.55

Attenuation Measurements by X-ray

The final step is practical since, using the x-ray machine supplied by the German company(PHYWE) , We performed X-ray attenuation measurements for samples of alloy A and B. All measurements were made at room temperature. The device operating voltage was 35 KV and the current was 0.2 mA.

Results and discussion

EDX testing

The elements involved in the preparation of alloys A and B under study were Specify using an EDX spectrometer, which works on the basis of electronic beam excitation and measurement of the energy of the radiation emitted by the samples under study, as shown in Fig.1 and 2. Tables 2 and 3 show the percentages of the atomic weight of an element after the alloys have been prepared.

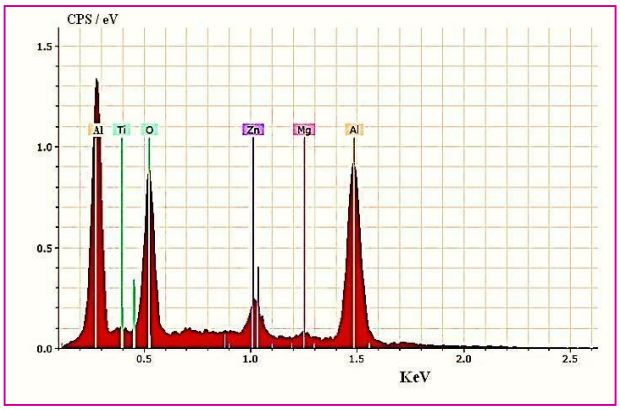

Figure 1. EDX spectrum of alloy A.

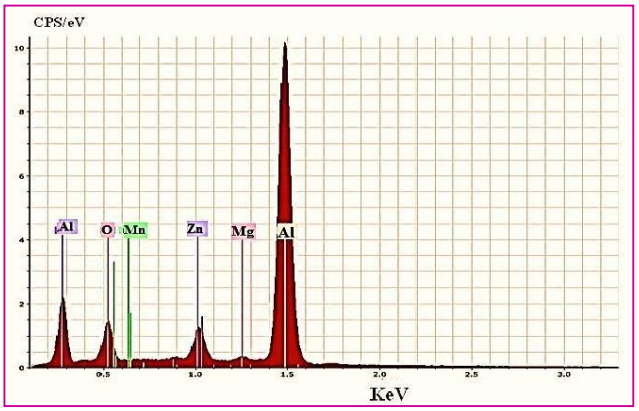

Figure 2. EDX spectrum of alloy B.

Table 2. The percentages of the atomic weight of an element after the alloy A.

El.	AN.	Series	Unn.C. Wt.%	Norm.C. Wt.%	Atom.C. (at.%)	Error	(1Sigma) (Wt.%)
Al	13	K	85.00	89.824	69.64		4.17
Zn	30	L	4.10	7.902	20.75		2.14
Mg	12	K	5.79	0.711	3.58		0.40
Ti	22	L	5.65	0.573	1.03		11.75
O	8	K	5.70	1.049	5.00		8.68
		Total :	106.24	100.00	100.00		

Table 3. The percentages of the atomic weight of an element after the alloy B.

El.	AN.	Series	Unn.C. (Wt.%)	Norm.C. (Wt.%)	Atom.C. (at.%)	Error	1Sigma) (Wt.%)
Al	13	K	73.88	82.222	75.82		2.17
Zn	30	L	5.84	8.114	11.85		0.52
Mg	12	K	0.75	1.591	1.76		0.10
Mn	22	L	0.68	1.663	1.53		0.51
O	8	K	5.70	6.20	8.95		1.19
		Total :	86.85	100.00	100.00		

XRD-testing

Japanese-made XRD-7000 gadget (40 Kv and 30mA) was utilized to evaluate the alloys for the creation of compounds. Fig. 3 shows the results of the experiments, which all took place at room temperature and ranged (10-80) degrees in angle, and other internationally accepted standards JCPDS were used to evaluate the collected data and findings tables 4 and 5. Alloys under investigation were tested for structural characteristics and X-ray attenuation coefficients in these tests.

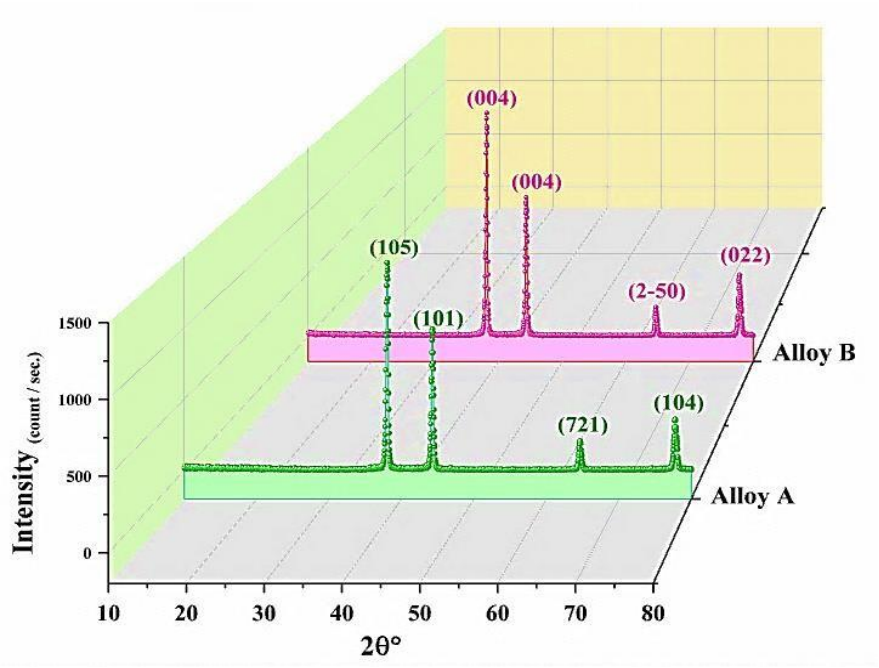

Figure 3. XRD spectrum

Table 4. Structural properties of alloy A from XRD spectrum.

Component phase	Crystal system	space group	(hkl)	d(A◦)	JCPDS No.
$AlMg_2Zn_{11}$	Hexagonal	(P-6m2)	(105)	2.36458	00-031-0024
TiO	Hexagonal	(P-6m2)	(101)	2.04453	01-082-0803
$Al_{12}Mg_{17}$	Cubic	(1-43m)	(721)	1.44084	01-073-1148
$AlTi_3$	Hexagonal	(P63/mmc)	(104)	1.22703	00-014-0451

Table 5. Structural properties of alloy B from XRD spectrum.

Component phase	Crystal system	space group	(hkl)	d(A◦)	JCPDS No.
Mn_2O_3	Cubic	(I-a3)	(004)	2.36166	01-071-0636
$MgAl_2O_4$	Cubic	(Fd3m)	(004)	2.04284	01-075-0711
$Al_{11}Mn_4$	Anorthic	(P-1)	(2-50)	1.43984	00-047-1272
$AlMg_2Zn_{11}$	Hexagonal	(P-6m2)	(022)	1.22633	00-031-0024

1. An calculation 1 was used to find association between the samples thickness and the absorbance. It is shown in Fig. 4 that with increasing thickness, x-ray absorbed by alloys under research increase, and that the slope of a straight line shows μ, which corresponds to [3,5,7] for other materials. Fig. 5 which depicts the association between the absorbance and the samples equivalent thickness under studied, shows that the link is direct and that the slope of the straight-line shows μ_m, which corresponds to [5,7] for other materials.
2. Fig. 6 and 7 show an converse correlation between the thickness of alloys A and B with (μ and μ_m) respectively, which is consistent with [4,5] for other studies and materials.
3. According to equation 3, the free path rate (linear and mass) has an inverse relationship with (μ and μ_m), respectively. We can see from Figs. 8 and 9 that the relationship between the free path rate and the thickness of samples is direct for both alloys under study, and this corresponds to With [8] for other studies and materials.
4. Further fig. 10 and 11 show association the half thickness HVL resultant from equation 4 with the thickness for both alloys under study. We notice the direct association, which indicates that upturning the sample's thickness upturns half the thickness of HVL, reducing the x-ray to half its value this corresponds to With [3,4] for other studies and materials.
5. If we look closely at figs. 4 to 11, we can see that Alloy A performs better in terms of radiation absorption than Alloy B. The absorption rate of alloy A is greater (0.59%) than that of alloy B. This is due to the result of the presence of (Ti) in alloy A and the appearance of the phases shown in Fig. 3 which enhanced the physical properties of alloy A and the enhanced radiation absorption [14]. This does not mean that Alloy B is not good in terms of attenuation, but its efficiency was lower than Alloy A because of the phases that appeared after its preparation as shown in Table 4 and 5.
6. Tables 6 and 7 include practical values of (μ, μ_m) calculated from the slope of the relationship between the logarithm of absorbance and the thickness of the samples and their equivalent thickness in Figs. 4 and 5, and practical values of (λ, λ_m, $X_{1/2}$, $X_{(m)1/2}$) calculated from the inverse relationship of (μ, μ_m) for X-rays, as well as theoretical values of (μ, μ_m, λ, λ_m, $X_{1/2}$, $X_{(m)1/2}$), Standard Deviation and Relative Standard Deviation for alloys A and B.

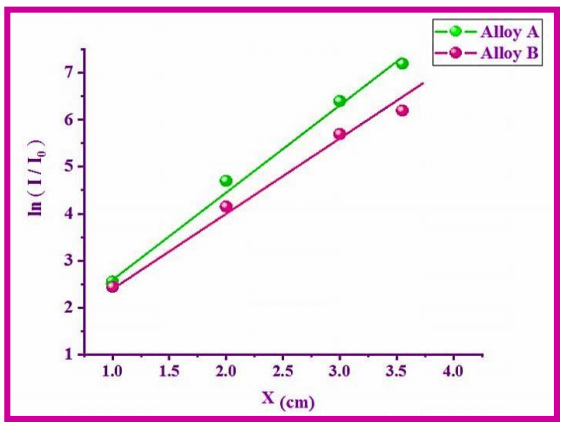

Figure 4. The relationship between the absorbance logarithm and the thickness of alloys (A &B).

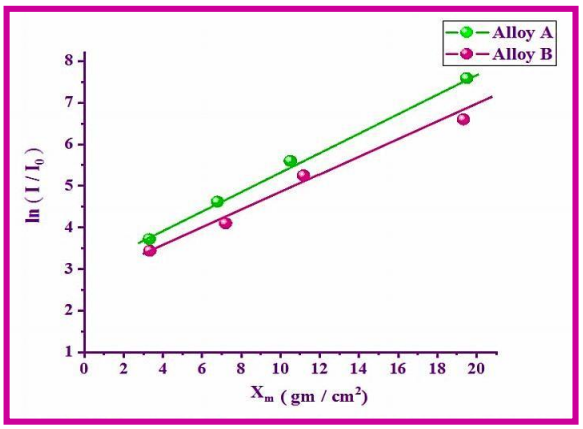

Figure 5. The relationship between the absorbance logarithm and the equivalent thickness of alloys (A &B).

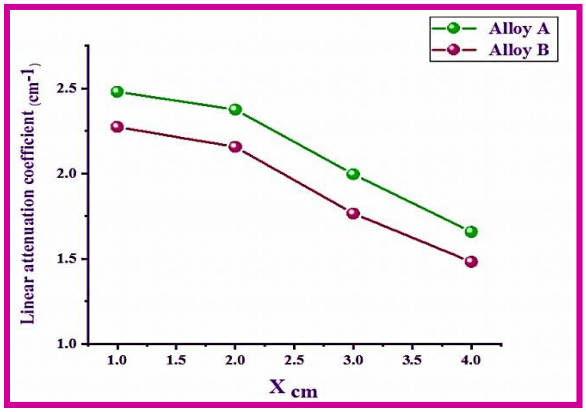

Figure 6. The relationship between linear coefficient attenuation and thickness of alloys (A &B).

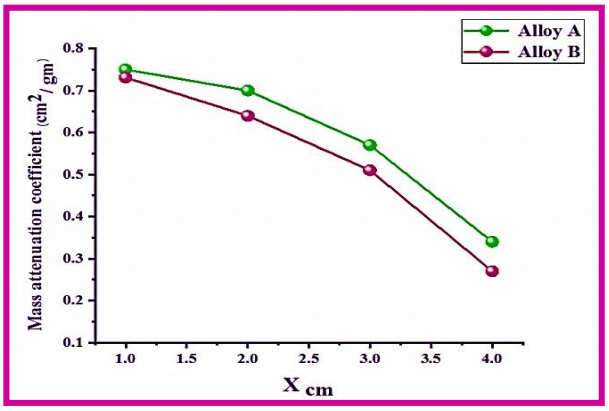

Figure 7. The relationship between mass coefficient attenuation and thickness of alloys (A &B).

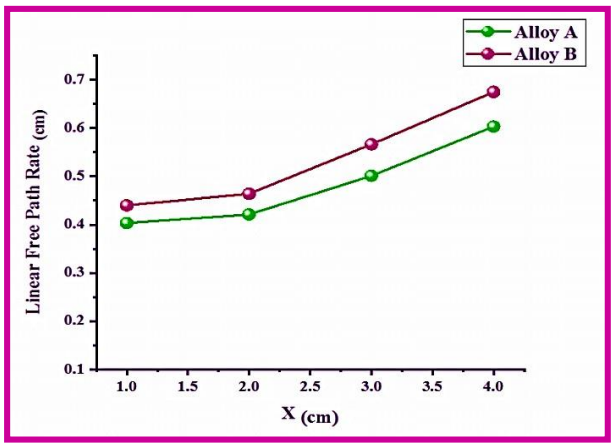

Figure 8. The relationship between linear free pathrate and thickness of alloys (A &B).

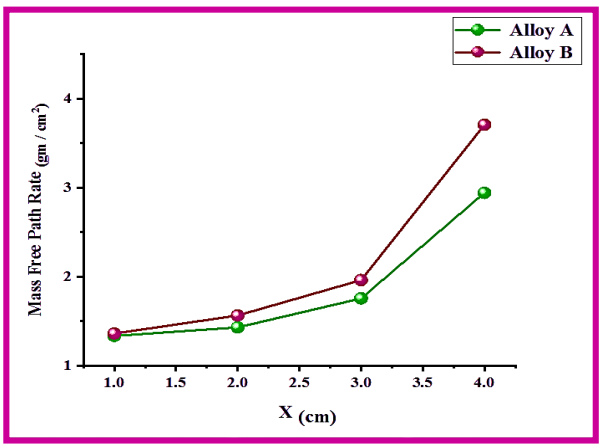

Figure 9. The relationship between mass free path rate and thickness of alloys (A &B).

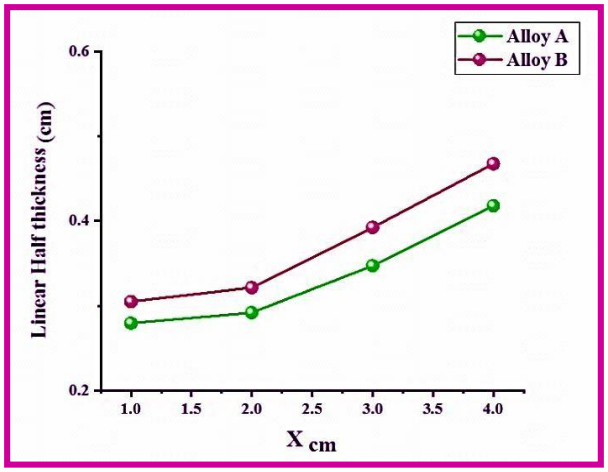

Figure 10. The relationship between linear half and thickness of alloys (A &B).

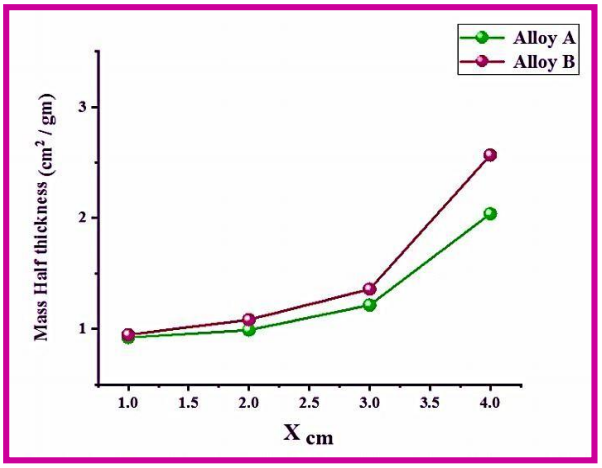

Figure 11. The relationship between mass halft thickness and thickness of alloys (A &B

Table 6. Experimental and theoretical values for (μ, μ_m, λ, λ_m, $X_{1/2}$, $X(m)_{1/2}$), Standard Deviation and Relative Standard Deviation for alloy A

Alloy A	Experimental		Theoretical	
	Av.$(x \pm \sigma x)$	$R.S.D = \left[\frac{\sigma(X)}{\bar{X}}\right] \times 100\ \%$	(x) Av.	$\text{Error} = \frac{\text{Theo.} - \text{Exp}}{\text{Theo.}} \times 100$
μ	2.1271±0.639499	17.669%	2.1289	0.000846
μ_m	0.5600±0.108029	31.037%	0.5851	0.042899
λ	0.4701±0.044018	18.936%	0.4697	0.00085
λ_m	1.7857±1.380123	39.71%	1.7091	0.04482
$X_{1/2}$	0.3257±0.02115	18.943%	0.3255	0.00061
$X_{(m)1/2}$	1.2375±0.660667	39.698%	1.1844	0.04483

Table 7. Experimental and theoretical values for (μ, μ_m, λ, λ_m, $X_{1/2}$, $X(m)_{1/2}$), StandardDeviation and Relative Standard Deviation for alloy B.

Alloy B	Experimental		Theoretical	
	Av.$(x \pm \sigma x)$	$R.S.D = \left[\frac{\sigma(X)}{\bar{X}}\right] \times 100\ \%$	(x) Av.	$\text{Error} = \frac{\text{Theo.} - \text{Exp}}{\text{Theo.}} \times 100$
μ	2.055±0.747404	18.9494%	2.0572	0.001069
μ_m	0.5377±0.107658	37.2329%	0.5389	0.002227
λ	0.4866±0.057642	20.051%	0.4861	0.00103
λ_m	1.8598±2.285758	49.770%	1.8556	0.00226
$X_{1/2}$	0.33722±0.27684	20.054%	0.3368	0.00125
$X_{(m)1/2}$	1.2888±1.090682	49.593%	1.2859	0.00226

Conclusion

1. Alloys A and B are Polycrystalline.
2. The relationship between the logarithm of absorbance with thickness and equivalent thickness is linear.
3. The relationship (μ, μ_m) with the thickness of the samples is an inverse relationship while the relationship is linear for eachof (λ, λ_m, $X_{1/2}$, $X(m)_{1/2}$) with the thickness of alloys A and B
4. The absorbance of alloy A is better than that of alloy B at a rate of (0.59%) for the same weight ratios of the components included in the composition of the alloys. This is due to the presence of Ti in the composition of alloy A, which gave good structural properties for absorbing X-rays.

References

1. Farid MM, Raed NR, Sokayna EY**.**Effect of Oxidation of Some Aluminum Alloys on X-ray Attenuation Coefficients.JMAUC.2012;4(1):33-47.
2. Isra' a MH , Laith AN. Studying the Linear and the Mass Attenuation Coefficient of Gamma Rays for Certain BuildingMaterials used in Iraq.RJS.2014;24(3):75-85.
3. Orhan G, Urkiye AT. Determination of Radiation Shielding Properties of Some Polymer and Plastic Materials againstGamma-Rays. ICCESEN.2016;130(1): 236-238
4. Akkas A. Determination of the Tenth and Half Value Layer Thickness of Concretes with Different Densities.APMAS.2016;.129(4):770-772.
5. Almeida TA, Nogueira MS, Vivolo V, Potiens MPA, Campos LL. Mass attenuation coefficients of X-rays in different baritеconcrete used in radiation protection as shielding against ionizing radiation. Radphyschem.2017;140:349-354.
6. Bashter II, Salem SM, Mansour SF, Sadeq MS, Mostafa AG, Saudi HA. Gamma Ray Attenuation Parameters of Some Boro-Silicate Glasses Doped Mixed Heavy Metal ions. BFS-ZU.2018;2018(1):18-24.

7. Karriman R, Seham AS, Hassan M F, Tartor BA, Ibrahim B. Characteristics of Gamma- Radiation Shielding for Raw WoodMaterials Commonly Used in Egypt. Bulletin of Faculty BFS-ZU.2018;2018(1):1-8.
8. Ahmed JM, Riyadh MR, Raed MS. Calculate the Attenuation of X-ray radiation for low density polyethylene compositeswith oyster shells powder extracted from the Caspian Sea in Iran. AJSRP.2019;3(1):38-49.
9. Nabil Janan Bahnam. Study the Effect of Scattering and Disperse Radiation on Equivalent Dose Rate for Al & Pb Shields.Baghdad Sic.J.2011;8(2):261-268.
10. Nagaraja N, Manjunatha HC, Seenappa L, Sathish KV, Sridhara KN ,Ramalingam HB. Gamma, X-ray and neutron shieldingproperties of boron polymers.IJPAP.2020;58:271-276.
11. Hayder SH, Abdel HA, Harith IJ. Dependence of gamma-ray absorption coefficient on the size of lead particle. BaghdadSic.J.2011;8(2):613-617.
12. Norman DC. Models of the Atomic Nucleus . 2nd Ed. Heidelberg : Springer ,2010. 6, The Mean Free Path of Nucleons inNuclei; 89.
13. William N, Barry M. Essential Statistics. 2nd Ed. McGraw Hill Higher Education,2017.5, Mean, median, mode, variance &standard deviation;410.
14. Sokayna EY, Mohammed MM, Abdulkader AA. Crystal Diffraction Techniques Were Used to Investigate the Structural Properties of Some Aluminum Alloys. ICAUC_ES.2022;961:1-9.